

Selective Alkane Hydroxylation in a Fluorous Solvent System Catalyzed by a Fluorocarbon-Soluble Transition-Metal Catalyst

Yuma Morimoto,* Yuki Shimaoka, Kosuke Fukui, and Shinobu Itoh*

Cite This: *ACS Omega* 2024, 9, 23624–23633

Read Online

ACCESS |



Metrics & More

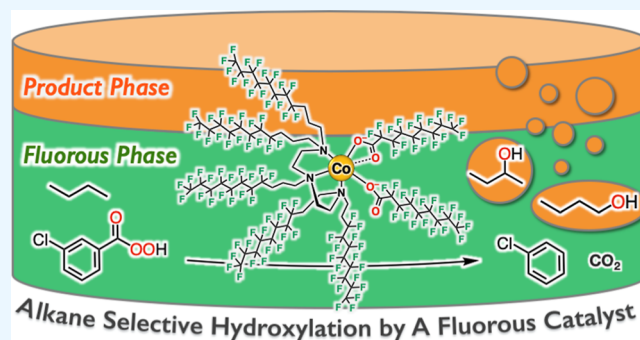


Article Recommendations



Supporting Information

ABSTRACT: Hydroxylation of aliphatic hydrocarbons requires highly reactive oxidants, but their strength can lead to undesired oxidation of the initially formed alcohols and solvents, undermining the product selectivity. To address these problems, we developed a novel catalytic system using fluorocarbon solvents. A cobalt complex supported by the fluorinated ligand, *N,N,N',N',N''*-pentakis- $[\text{CF}_3(\text{CF}_2)_7(\text{CH}_2)_3]$ -diethylenetriamine (Rf-deta), acts as an efficient catalyst [turnover number (TON) = 1203, turnover frequency = $51 \pm 1 \text{ min}^{-1}$] for cyclohexane hydroxylation with the *m*-chloroperbenzoic acid oxidant, achieving high alcohol selectivity (96%). Overoxidation to form cyclohexanone is minimized due to the separation of cyclohexanol from the reaction phase, comprising perfluoromethylcyclohexane and α,α,α -trifluorotoluene. The catalyst hydroxylates primary carbons (5 examples) and exhibits significant reactivity toward the terminal C–H bond of normal hexane (TON = 13). This system extends to the hydroxylation of the gaseous substrate butane, yielding the corresponding alcohols.



INTRODUCTION

Selective hydroxylation of the $\text{C}(\text{sp}^3)\text{--H}$ bond is a challenging reaction due to the much lower reactivity of the C–H bonds in the substrates than those of the alcohol products.¹ Overoxidation of the alcohol products to carbonyl compounds decreases the alcohol selectivity. Furthermore, solvent oxidation decreases the reaction efficiency when highly oxidative reagents are employed.² These problems become inevitable when we try to oxidize inert alkane substrates, in particular, primary carbon substrates with high C–H bond dissociation energy. In this respect, water is an attractive solvent as it is resistant to oxidative attack.³ However, the immiscibility of hydrocarbon substrates under aqueous solvent conditions is another problem.

One potential solution to these challenges involves the employment of perfluorocarbons (PFCs) as solvents due to their exceptional resistance to oxidation reactions, imparted by the inherent stability of C–F bonds.⁴ Recently, Ohkubo and Hirose utilized perfluorohexane as a solvent in their photocatalytic methane oxidation system, which featured chlorine radicals (Cl^\bullet) as the reactive species.⁵ We employed α,α,α -trifluorotoluene (TFT) to elongate the lifetime of an oxoiron(IV) porphyrin radical cation species (so-called compound I) and demonstrated its reactivity toward primary carbon substrates.⁶ Even in the presence of highly reactive oxidants, the fluorocarbon solvent did not disturb the oxidation reactions.

In addition to enhancing chemical stability, the introduction of fluorine atoms to solvent molecules significantly decreases

their miscibility with polar organic compounds such as alcohols.⁷ This characteristic immiscibility of PFCs and alcohols can be exploited as a promising strategy for improving the alcohol product selectivity in alkane hydroxylation reactions. The product alcohols escape from the reaction phase and thus do not suffer from the overoxidation (Scheme 1).

Typical metal-ion complexes are, however, poorly soluble in PFC solvents. Nevertheless, Horváth and Rábai succeeded in solubilizing a rhodium complex as a hydroformylation catalyst in PFC using ligands bearing fluoroalkyl chains.⁸ A fluorous phase containing the Rh catalyst and an organic phase containing a substrate are miscible in a hand-warmed condition ($>36^\circ\text{C}$). A decrease in the solution temperature induces spontaneous phase separation again. The repeatable phase association and separation allow recycling of the Rh catalyst by simple decantation. Since then, transition-metal (Mn, Co, Cu, and Pd) complexes bearing fluorocarbon chains have been applied to oxidation reactions in PFC solvent systems.⁹ For instance, Fish et al. investigated cyclohexane hydroxylation with *tert*-butyl hydroperoxide (*t*BuOOH) under

Received: February 6, 2024

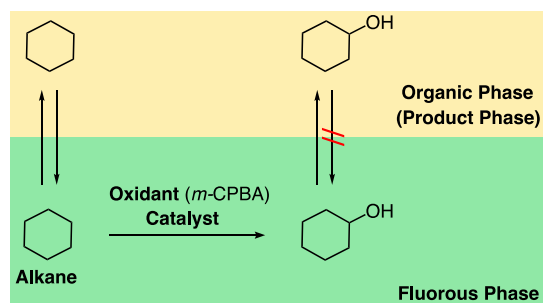
Revised: April 26, 2024

Accepted: May 14, 2024

Published: May 23, 2024



Scheme 1. Strategy of This Work to Achieve High Alcohol Selectivity with a Transition-Metal Complex Anchored in a Fluorous Phase



aerobic conditions using a biphasic system consisting of a fluorous phase (perfluoroheptane) and an organic phase (substrate itself) with fluorocarbon-soluble transition-metal complexes. In their study, alcohol product selectivity was up to 60%, probably because the radical chain reactions indiscriminately oxidized the substrate and the alcohol product (Scheme S1 in Supporting Information).⁹¹

We herein report a selective alkane oxygenation system that features cobalt catalysts bearing a ligand functionalized with fluoroalkyl chains (Figure 1). The fluorous ligand confined

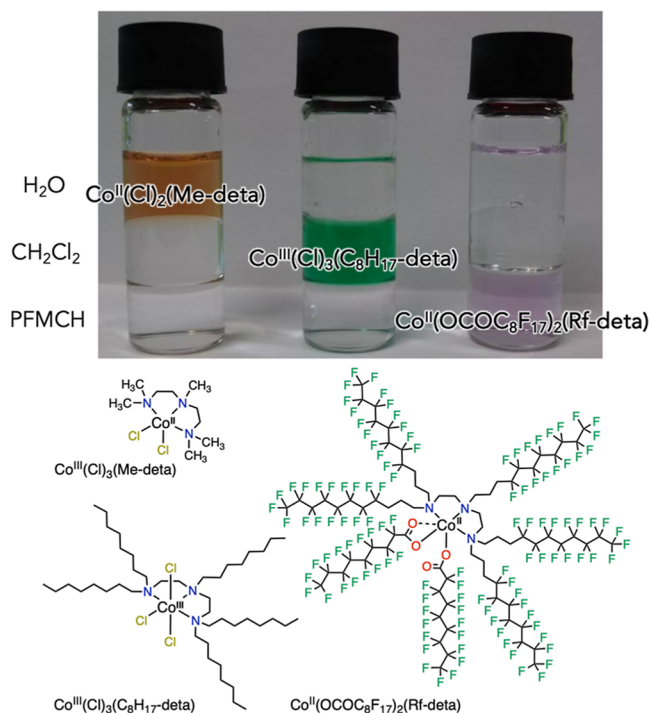


Figure 1. Demonstration of the solubility of the cobalt complexes supported by the Me-deta (left bottle), C₈H₁₇-deta (middle bottle), and Rf-deta (right bottle) ligands into water, dichloromethane, and PFMCH.

them to the fluorous solvent phase consisting of perfluoromethylcyclohexane (PFMCH) and TFT. The catalytic activity of the fluorinated complex was examined in cyclohexane hydroxylation with *m*-chloroperbenzoic acid (*m*-CPBA) in the fluorous solvent at 50 °C. At the initial stage of the catalytic reaction, the system was monophasic, consisting of the complex catalyst, the substrate, and the

fluorocarbon solvent. Subsequently, the alcohol product separated from the fluorous phase to form a biphasic system as the catalytic reaction proceeded. Reported together is the scope of applicable alkane substrates, including primary carbon and the gaseous substrate *n*-butane.

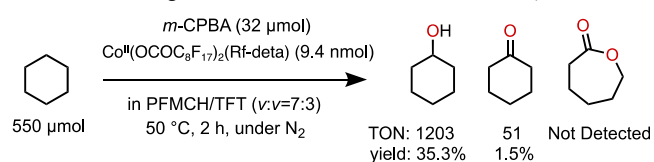
RESULTS AND DISCUSSION

Synthesis of a Cobalt-Complex Soluble to Fluorous Solvents.

Fluoroalkyl chains of the ligand were introduced by the reaction of diethylenetriamine and CF₃(CF₂)₇(CH₂)₃I by following reported procedures.^{9e,1} A cobalt(II) salt Co₂(OCOC₈F₁₇)₄[(CH₃CH₂)₃NH·OCOC₈F₁₇](H₂O)₈, containing perfluorononanoate counteranions and triethylamine (for ¹H NMR, Figure S1), was prepared following the synthetic procedures for the preparation of copper(II) salt, Cu₂(OCOC₈F₁₇)₄.¹⁰ The metal salt did not show high solubility in PFMCH. However, they were immediately solubilized by treatment with the fluorinated ligand (Figure 1), upon which a change in the color of the solution was observed, indicating formation of the corresponding transition-metal complex. Both the fluoroalkyl chains on the ligands and the fluorinated counteranion facilitate solubilization of the complexes into PFMCH and prohibit their dispersion into the other phases. For example, Co^{II}(OCOC₈F₁₇)₂ (Rf-deta) remained in the PFMCH phase, whereas the cobalt complexes with pentamethyldiethylenetriamine (Me-deta) and pentaocetylthyltriethylenetriamine analogue (C₈H₁₇-deta) ligands bearing normal alkyl chains were only soluble in water and CH₂Cl₂ phases, respectively. The PFMCH phase containing Co^{II}(OCOC₈F₁₇)₂(Rf-deta) was separated from cyclohexanol while being able to retain cyclohexane (Figure S2).

Comparison of the Catalytic Activities of Co^{II} Complexes in Cyclohexane Hydroxylation Using *m*-CPBA. The catalytic ability of the cobalt complexes for cyclohexane hydroxylation was examined using *m*-CPBA (Scheme 2). A partially fluorinated solvent, α,α,α-trifluor-

Scheme 2. Catalytic Hydroxylation of Cyclohexane by *m*-CPBA Catalyzed by a Cobalt Catalyst Supported by a Fluorinated Ligand in a Fluorocarbon Solvent System



otoluene, was necessary to solubilize *m*-CPBA in PFMCH, although its miscibility with cyclohexanol will decrease the separation coefficient of produced alcohol from the reaction system. The reaction was initiated by *m*-CPBA addition into a PFMCH/TFT solution containing the substrate and the complex prepared in situ by mixing the ligand and the metal salt under an inert atmosphere at 50 °C. The hydroxylation of cyclohexane proceeded with a turnover number (TON) of 1203 and markedly high alcohol product selectivity (>96%) over ketone and ε-caprolactone. No chlorocyclohexane or fluorocyclohexane were detected. Table S1 summarizes the influence of the mixing ratio of PFMCH/TFT and reaction temperature. The selectivity for cyclohexanol produced in this study represents the highest value reported to date when compared with that of other examples for cyclohexane hydroxylation (Table S2). The alcohol product selectivity is

remarkable when compared to the autoxidation of alkanes with *t*BuOOH and oxygen (O₂) in a substrate/fluorinated solvent biphasic catalyst system (TON: 12.5, alcohol selectivity: 56%).^{9e,h,m} In the absence of the Rf-deta ligand, the catalytic efficiency was significantly decreased: TON for cyclohexanol formation was 36 and only a trace amount of cyclohexanone was observed.

Interestingly, after the catalytic reaction, we could observe a spontaneous phase separation of the final reaction mixture in a Pasteur pipet (Figure 2), where cyclohexanol formed a new

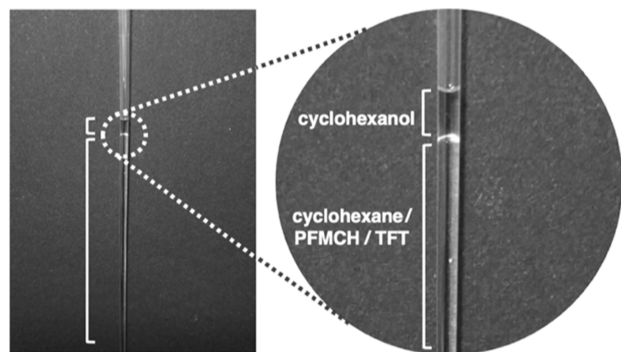


Figure 2. Separation of the cyclohexanol product from the fluororous reaction phase after the catalytic reaction.

phase on the PFMCH/TFT/cyclohexane phase. To corroborate this result, we evaluated the cyclohexanol solubility in the PFMCH/TFT/cyclohexane mixture (700/300/300 μ L) with *m*-CPBA at 50 $^{\circ}$ C. The resultant mixture after the catalytic reaction was reproduced by adding 5.0 μ L (47 μ mol) of cyclohexanol to the PFMCH/TFT/cyclohexane mixture. After the solution was left to stand at 50 $^{\circ}$ C with steering, only 30 μ mol of cyclohexanol was detected by its gas chromatograph-flame ionization detector (GC-FID) analysis (Table S3). This result indicated that a portion of the produced cyclohexanol escaped from the reaction phase during the catalytic reaction. Consequently, this escape phenomenon leads to a reduction in the effective concentration of cyclohexanol surrounding the catalyst within the experimental setup described above. The observation of phase separation in the reaction mixture was further corroborated by dynamic light scattering (DLS) analysis. Notably, the injection of 2.0 μ L of cyclohexanol into a solution comprising PFMCH/TFT/cyclohexane (700/300/300 μ L) resulted in the emergence of a peak at around a diameter of 160 nm. This newly formed peak can be attributed to the presence of small droplets primarily composed of cyclohexanol that escaped from the reaction phase (Figure S3a).^{11–13}

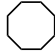
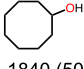
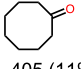
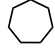
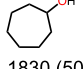
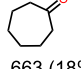

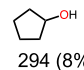
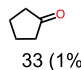
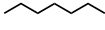
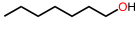
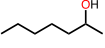
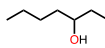
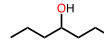

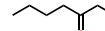
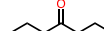
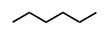

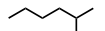
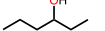
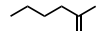
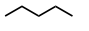
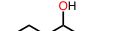
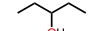
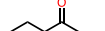
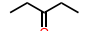
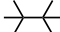
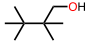
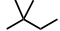
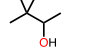
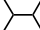
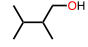
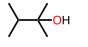
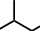
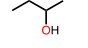
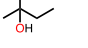

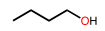
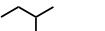

Substrate Scope: C5–C8 Alkanes. The substrate scope was investigated using various alkanes under the optimized reaction conditions (Table 1). In the case of cyclooctane and cycloheptane, the catalyst system produced corresponding alcohols as the major products with a high TON (up to 1800) and a relatively high alcohol selectivity (74–82%) (entries 1 and 2). The higher TONs obtained in the oxidation of cyclooctane and cycloheptane can be ascribed to their lower bond dissociation energies of the C–H bonds (95.7 and 94.0 kcal mol⁻¹, respectively) compared to that of cyclohexane (99 kcal mol⁻¹). The higher TON for alcohol production, facilitating the overoxidation, resulted in lower alcohol selectivity, as discussed later (Solvent Effects section). The

catalytic activity decreased (TON \approx 300) in the oxidation of cyclopentane, although cyclopentane has C–H bonds (95.6 kcal mol⁻¹) that are weaker than those of cyclohexane (entry 3). We examined the reaction-inhibition effect of cyclopentanol on the optimized system for cyclohexane hydroxylation to elucidate the reason for this. The addition of cyclopentanol (5% of the amount of cyclohexane, 11 mM) drastically decreases the TON for cyclohexanol formation by about 10-fold (Table S4). Cyclopentanol has a smaller ligand cone angle than those of C6–C8 cyclic alcohols and probably binds to the metal center strongly in the nonpolar solvent system. The inhibition by produced alcohol is reasonable, considering the slow ligand exchange of Co(III) complexes in a low-spin state.

This system was applicable to the oxidation of *n*-alkanes to demonstrate that secondary alcohols were mainly produced with an alcohol selectivity of 72–95% (entries 4–6). Lower *n*-alkane substrates appeared to form fewer products. Remarkably, primary alcohol products were also produced despite the very high dissociation energies of the primary C–H bonds (\approx 100 kcal mol⁻¹), although the yields were lower than those of the secondary alcohol products. The TON of 13 for terminal C–H hydroxylation with *n*-hexane was the highest value among the reported molecular catalyst systems in thermal conditions (Table S5). In the system presented here, suppression of solvent oxidation effectively induced the formation of primary alcohol products. We further examined the ability of this reaction system to cleave primary C–H bonds using 2,2,3,3-tetramethylbutane, where the TON of the reaction was 42 (entry 7). Hydroxylation of other branched hydrocarbons such as 2-methylbutane, 2,2-dimethylbutane, and 2,3-dimethylbutane yielded secondary and tertiary alcohols without forming any ketone products (entries 8–10). The reason remains elusive for the lower yields of 2,2-dimethylbutane and 2-methylbutane hydroxylation compared to 2,3-dimethylbutane. Fine-tuning the ratio of solvents mixed or adjusting the reaction temperature may enhance both the TON and the selectivity of the reactions. However, we have not yet conducted a detailed optimization of these conditions for each individual substrate.

Oxidation of *n*-Butane. Under standard pressure conditions, the catalytic conversion of gaseous alkanes presents a considerable challenge owing to their low solubility in conventional solvents. Fluorocarbons, however, are recognized for their exceptional ability to incorporate lower-alkanes such as methane, ethane, propane, and butane efficiently.¹⁴ Accordingly, we attempted to hydroxylate *n*-butane by taking advantage of the high solubility of alkane gases in fluororous solvents. The solubility of butane in PFMCH at 25 $^{\circ}$ C was confirmed to be 310 mM, which is 10-fold higher than that in CH₃CN (29 mM at 25 $^{\circ}$ C) by ¹H NMR. The hydroxylation reaction of *n*-butane was performed using the PFMCH/TFT system (Table 1, entry 11) to yield 1- and 2-butanol and 2-butanone in 0.5, 8, and 4% yields, respectively (based on the oxidant), and a total TON of 477. Thus, this system showed a much higher TON than those reported values for butane oxidation under normal pressure conditions.¹⁵ This oxidation system also showed a reasonably high alcohol selectivity of 69%, even with the limited concentration of *n*-butane; the oxidation reactions of other substrates were carried out at much higher concentrations (2 M). In a control experiment using CH₃CN as the solvent, butanone was obtained as the sole product with a lower yield (3%) and a TON of 143 (entry

Table 1. Substrate Scope of the Catalytic System^f

entry	substrate	product				alcohol selectivity ^c
		TON ^a (yield ^b)				
1		 1840 (50%)	 405 (11%)			82%
2		 1830 (50%)	 663 (18%)			73%
3		 294 (8%)	 33 (1%)			90%
4		 26 (1%)	 438 (12%)	 575 (16%)	 184 (5%)	92%
		 50 (1%)	 47 (1%)	 14 (0.4%)		
5		 13 (0.4%)	 262 (7%)	 265 (7%)	 26 (1%)	95%
6		 252 (8%)	 37 (1%)	 47 (1%)	 63 (2%)	72%
7			 42 (1%)			>99%
8			 41 (1%)			>99%
9		 102 (3%)		 958 (26%)		>99%
10		 48 (1%)		 53 (1%)		>99%
11 ^d [12 ^e]		 20 (0.5%), [<1 ($<1\%$)]	 311 (8%), [<1 ($<1\%$)]	 146 (4%), [143 (3%)]		69%, [0%]

^aDetermined by GC-FID (entries 1–6) or ¹H NMR (entries 7–12). ^bCalculated based on *m*-CPBA added. ^c(μmol of alcohol)/(μmol of alcohol and ketone). ^dButane saturated (310 mM). ^eIn CH₃CN/cosolvent (v/v = 3:7), butane saturated (29 mM). ^fConditions; substrates: 550 μmol (2 M), *m*-CPBA: 32 μmol , Co₂(OCOC₈F₁₇)₄((CH₃CH₂)NH₂OCOC₈F₁₇)(H₂O)₈; 4.9 nmol, Rf-deta: 9.4 nmol in TFT/cosolvent (3:7) under N₂ at 50 °C for 2 h. TON is calculated based on the amount of Rf-deta.

12). The decrease of TON in the CH₃CN system is ascribed to the lower solubility of butane. The disappearance of alcohol selectivity is due to the miscibility of the alcohol product to the reaction system. Alcohol selectivity was also decreased in the cyclohexane hydroxylation reaction in the CH₃CN-based solvent system (vide infra).

Mechanistic Studies. Extensive research attention has been directed toward the inert alkane hydroxylation reaction by *m*-CPBA catalyzed by transition-metal complexes.^{2b,16} Here, we conducted a concise investigation of the reaction mechanism. Upon the addition of *m*-CPBA to the reaction solution, the Co^{II} starting complex underwent rapid oxidation to a Co^{III} species. This transformation was confirmed by the disappearance of the EPR signal due to the Co^{II} species (Figure S4). The cobalt Co^{III} species showed an electronic

absorption band at 600 nm (with an extinction coefficient, ϵ , of approximately 50 M⁻¹ cm⁻¹, ascribed to ¹T_{1g} ← ¹A_{1g} transition), persisting throughout the catalytic reaction process.¹⁷

The amounts of the products (cyclohexanol and cyclohexanone) increased linearly following zeroth-order kinetics, and the turnover frequency reached its maximum value of 51 ± 1 min⁻¹ in the presence of the highest substrate concentration (Figure 3a). The reaction rates (V , $\mu\text{mol min}^{-1}$) obtained from the slopes of the plot showed proportional dependence on the concentration of cyclohexane and the cobalt complex, while they showed no dependence on the *m*-CPBA concentration (Figure 3b–d). Therefore, the rate equation was determined as eq 1, where k indicates the second-order reaction-rate constant (24 ± 1 M⁻¹ min⁻¹).

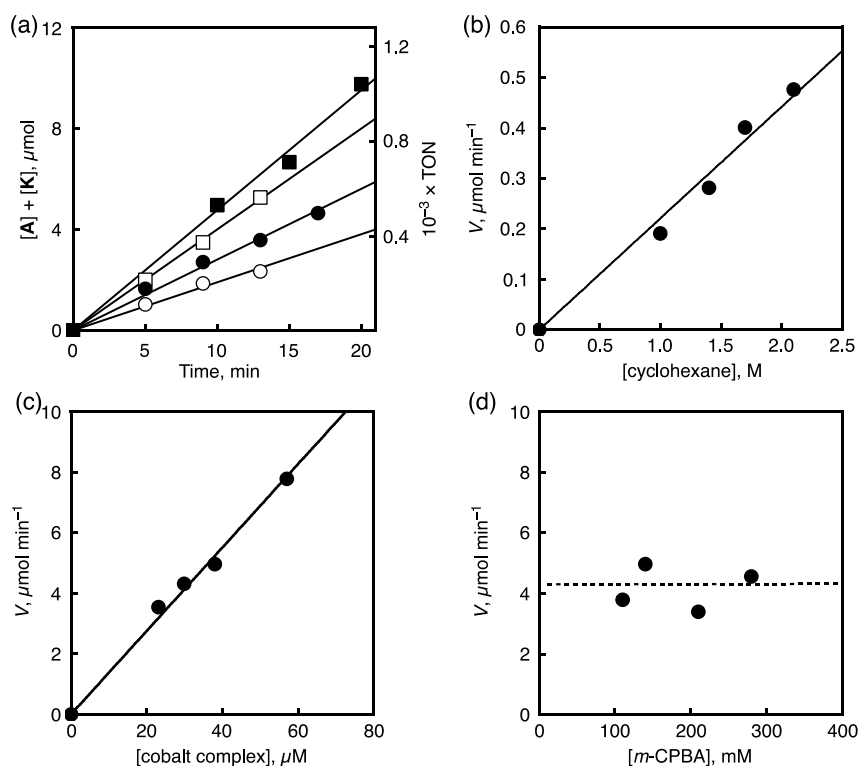


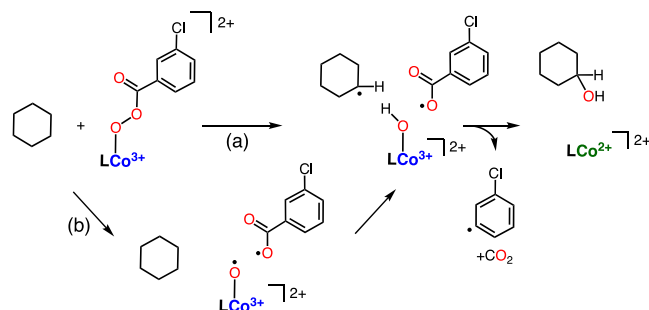
Figure 3. (a) Time-course of product formation [cyclohexanol (A) and cyclohexanone (K)] for catalytic hydroxylation of cyclohexane (closed square: 2.1 M, open square: 1.7 M, closed circle: 1.4 M, open circle: 1.0 M) by *m*-CPBA (0.14 mM) catalyzed by the Co^{II} Rf-deta complex (36 μM) in a PFMCH/TFT mixed solvent system under N₂ at 50 °C. (b) Plot of the reaction rate (V , μmol min⁻¹) against the cyclohexane concentration. (c) Dependence of V on the concentration of the cobalt complex in the presence of cyclohexane (2.1 M) and *m*-CPBA (0.14 M). (d) Dependence of V on the concentration of *m*-CPBA in the presence of cyclohexane (2.1 M) and the cobalt complex (36 μM). The sum of molar amounts of A and K were used to calculate TON and V values.

$$V = k[\text{substrate}][\text{cobalt complex}] \quad (1)$$

This equation indicates that the turnover-limiting step (TLS) of the catalytic cycle includes a reaction of the reactive intermediate based on a cobalt complex with the substrate. A deuterium kinetic isotope effect (KIE) value of 49 was obtained when using cyclohexane-*d*₁₂ instead of cyclohexane.¹⁸ This considerable KIE value is consistent with the involvement of hydrogen abstraction from the substrate in TLS of the catalytic reaction. In all cases listed in Table 1, chlorobenzene is generated as a byproduct from *m*-CPBA, which indicates that the cobalt complex facilitates the O–O bond homolysis of *m*-CPBA.

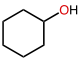
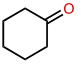
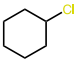
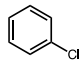
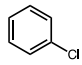
Experimental results indicate that the TLS of the catalytic reaction is a concerted process: the O–O homolysis of a Co^{III}-(*m*-CPBA) complex that is synchronous with the C–H bond activation step of the substrate (Scheme 3a). Such a concerted process was suggested in a Ni-acylperoxide system,^{16k} recently investigated in a Co-acylperoxide system,¹⁹ and the alkane hydroxylation reaction by *m*-CPBA without a metal catalyst.²⁰ This type of concerted mechanism is also investigated in the sp³-C–H bond activation reaction by Cu-alkyl peroxido and Fe-acyl peroxido complexes.^{16c,21} An alternative mechanism involves a stepwise process: the initial formation of a Co^{III}-oxyl (or formally Co^{IV}-oxido) complex, followed by the oxidation of the substrate (Scheme 3b). However, when following path B, the Co^{III}-oxyl species becomes the prominent component in the system, awaiting the TLS, which is inconsistent with the EPR results of the reaction mixture, denying the presence of EPR-active species. Considering the known instability of

Scheme 3. (a) Concerted O–O Bond and C–H Bond Activation and (b) stepwise O–O Bond Homolysis Followed by Hydrogen Atom Abstraction



hypervalent cobalt complexes, the concerted mechanism appears to be the more plausible explanation for this catalytic system.²² Nonetheless, the potential involvement of hypervalent cobalt complexes, which may rapidly react with the substrate upon formation, cannot be entirely ruled out.²³ The generated *m*-CBA radical through the O–O bond homolysis is known to lead to prompt decarboxylation to generate chlorophenyl radicals,^{2a} and this highly reactive radical species should instantly abstract hydrogen from the H–O group of another *m*-CPBA molecule (BDE_{O–H} ~ 96.5 kcal mol⁻¹), which is the best hydrogen donor in the reaction system (Scheme S2).^{24–26} The coordination of the *m*-CPBA radical [ClC₆H₄C(O)OO•] to the cobalt(II) complex regenerate the putative reactive intermediate, Co(III)(OOCOC₆H₄Cl) species to close the catalytic cycle. The free radical-based

Table 2. Effects of Cosolvents on the Catalytic Oxidation of Cyclohexane^c

entry	co-solvent	Hildebrand solubility parameter, δ (cal/cm ³) ^{1/2}	TON ^a					total	yield ^b (%)	alcohol select. ^c (%)
										
1	CH ₃ NO ₂	12.7	111	0	0	111	99	3	>99	
2	DMF	12.1	37	0	0	37	104	1	>99	
3	CH ₃ CN	12.0	1090	491	0	1580	1270	43	69	
4	CH ₃ CH ₂ CN	10.6	580	341	0	921	1050	25	63	
5	CH ₂ Cl ₂	9.9	1250	221	147	1470	1340	40	85 ^[d]	
6	C ₆ H ₅ Cl	9.6	609	91	57	700	–	19	87 ^[d]	
7	CHCl ₃	9.3	886	477	432	1360	808	37	65 ^[d]	
8	cyclohexane	8.2	1970	126	0	2100	1140	57	94	
9	PFMCH	6.0	1200	50	0	1250	1220	34	96	

^a(Amounts of products)/(amount of cobalt ion [9.8 nmol]). ^bYields determined based on *m*-CPBA added. ^c(μ mol of cyclohexanol)/(μ mol of cyclohexanol and cyclohexanone). ^d(μ mol of cyclohexanol)/(μ mol of cyclohexanol, cyclohexanone, and chlorocyclohexane). ^eConditions; cyclohexane: 550 μ mol, *m*-CPBA: 32 μ mol, Co₂(OCOC₈F₁₇)₄((CH₃CH₂)NH-OCOC₈F₁₇)(H₂O)₈: 4.9 nmol, Rf-deta: 9.4 nmol in TFT/cosolvent (v/v = 3:7) under N₂ at 50 °C for 2 h.

mechanism hardly explains the TON dependence on the substrate shown in Table 1, where cyclopentane with lower BDE values shows lower TON compared to that of cyclohexane or cyclooctane, as discussed above in the Substrate Scope: C5–C8 Alkanes section.

Solvent Effects. We next employed conventional organic solvents to investigate the effect of solvent on the alcohol product selectivity (Table 2). Because the Co-complex Co^{II}(OCOC₈F₁₇)₂(Rf-deta) was not soluble in pure organic solvents, TFT (30 vol %) was added to solubilize the complex in all the solvent systems. In polar solvent systems, dimethylformaldehyde (DMF)/TFT and CH₃NO₂/TFT, the cobalt complex could not exert its activity, and TONs were significantly lower than those obtained in the PFMCH system (entries 1 and 2). The nitrile solvent systems such as CH₃CN/TFT and CH₃CH₂CN/TFT facilitated the catalytic efficiency, but considerable amounts of ketone were produced, lowering the A/K (alcohol/ketone) values for those systems (entries 3 and 4). The halogenated solvent systems such as CH₂Cl₂/TFT, C₆H₅Cl/TFT, and CHCl₃/TFT improved the A/K value.²⁹ However, formation of chlorinated products reduced alcohol product selectivity (entries 5–7); chlorocyclohexane (Cl) was obtained in 10, 8, and 32% yields, respectively, most likely by the reaction between cyclohexyl radicals and chlorine radicals generated by the oxidation of the solvent. Formation of chlorinated products was also reported for hydroxylation reactions of cyclohexane and adamantane in halogen solvents, where hexachloroethane was obtained as a byproduct, although the detailed reaction mechanisms of these reactions remain unclear.^{2a,f} The formation of 1,1,2,2-tetrachloroethane and hexachloroethane for entries 5 and 7, respectively, was observed by GC-FID, confirming the occurrence of solvent oxidation in the halogen solvent systems. In contrast, no byproducts such as fluorocyclohexane were detected in the PFMCH/TFT mixed solvent system (entry 9). When the substrate (cyclohexane) itself was used as the cosolvent (cyclohexane/TFT, v/v = 7:3), a high alcohol selectivity was achieved (entry 8). In summary, the alcohol product selectivity tends to increase with a decrease of solvent polarity

parameterized by the Hildebrand solubility parameter (δ), as shown in Table 2.^{27,28}

Alcohol product selectivity is the result of the accumulation of the relative rate of alcohol oxidation and alkane oxidation (V_A/V_K), as described by the following equation

$$V_A/V_K = k_{\text{alkane}}[\text{alkane}]/k_{\text{alcohol}}[\text{alcohol}] \quad (2)$$

where k_{alkane} and k_{alcohol} indicate rate constants for alkane oxidation and alcohol oxidation, respectively. As shown by the equation, one of the determining factors of the alcohol product selectivity is the concentration ratio of alcohol to alkane around the reactive species. As demonstrated in Figure 2, the spontaneous separation of produced alcohol from the PFMCH/TFT solvent system should reduce the effective concentration of alcohol around the catalyst, leading to high-alcohol product selectivity. Equation 2 also explains the high-alcohol product selectivity observed in the cyclohexane/TFT system (entry 15), where the cyclohexane concentration is the highest. The ratio of k_{alkane} and k_{alcohol} can also be a determining factor of the product selectivity. However, the solvent polarity hardly has a significant influence on the rate of the C–H bond dissociation reaction, enough to explain the selectivity listed in Table 2.^{30,31}

CONCLUSIONS

In this work, we prepared a novel cobalt catalyst system soluble in PFMCH and assessed its efficiency toward cyclohexane hydroxylation with *m*-CPBA. The Co complex with Rf-deta affords a high TON and a high alcohol selectivity in cyclohexane hydroxylation reactions (1203 and 96%). The high selectivity toward alcohol products can be attributed to the immiscibility of the initial product, cyclohexanol, to the components of the reaction solution. The reaction system is applicable to the hydroxylation of cyclic and acyclic C5–C8 alkanes to form the corresponding secondary and tertiary alcohols. Remarkably, primary alcohols are also produced by the hydroxylation of the terminal carbons of 5 substrates. The characteristic solubility of gaseous hydrocarbons in fluororous solvent systems was exploited for the hydroxylation reaction of butane under normal pressure to yield 2-butanol and 1-butanol

with good selectivity without overoxidation of the alcohol products (sum of TON for 1-butanol and 2-butanol: 331, alcohol selectivity: 69%). Thus, this study presents the first example of a catalyst system that employs a fluorocarbon to achieve high alcohol product selectivity in catalytic alkane oxidation. Accordingly, this study presents a novel strategy for catalytic transformations of inert alkane substrates that require highly reactive oxidative species.

Fluorous solvents have the unique ability to dissolve higher concentrations of oxygen compared to conventional organic solvents.¹⁴ This property will be harnessed to facilitate the aerobic oxidation of substrate, a process that continues to pose significant challenges in the field of organic chemistry.³² The concept of this fluorous system can also inform the design of heterogeneous catalysts. By anchoring a fluorous environment onto the surface of solid support, we could replicate the benefits observed in our solution system while mitigating the environmental impact of fluorinated chemicals.³³

EXPERIMENTAL SECTION

Materials. The reagents and solvents used in this study were commercial products of the highest available purity. All solvents and all liquid substrates were dried over 4 Å molecular sieves (Nacalai Tesque, Inc.) activated by the standard procedure.³⁴ *m*-CPBA was purified by recrystallization from CH₂Cl₂ at 10 °C, and its purity was determined to be 90% by titration against NaI. In this manuscript, the actual amount of the *m*-CPBA added after considering its 90% purity is given. All other chemicals were used as received. PFMCH, *N,N,N',N',N''*-pentamethyldiethylenetriamine (Me-deta), 4,4,5,5,6,6,7,7,8,8,9,9,10,10,11,11,11-heptafluoroundecyl iodide (CF₃(CF₂)₇(CH₂)₃I), perfluorooctanoic acid (CF₃(CF₂)₆CF₂CO₂H), and butane gas were purchased from Tokyo Chemical Industry Co., Ltd. and were used as received. *N,N,N',N',N''*-Pentakis(CF₃(CF₂)₇(CH₂)₃)diethylene-tri-amine (Rf-deta) was prepared using previously reported procedures.^{9e,35} Solvents employed for catalytic reactions were dried with molecular sieves before use. Caution: Although no problems were encountered during complex synthesis, perchlorate salts are potentially explosive and should be handled with care.

Equipment. Fast atom bombardment mass spectroscopy (FAB-MS) was conducted with a JEOL JMS-700T Tandem MS-station mass spectrometer. The product mixtures resulting from the catalytic reactions were analyzed using a Shimadzu GC-2010 GC-FID equipped with a GL Science InertCapWAX capillary column (30 m × 0.25 mm), an AOC-20s auto sampler, and an AOC-20i auto injector or by ¹H NMR (400 MHz, JEOL ECS 400). The synthesis of metal salts and preparation of samples for catalytic reactions were performed in a glovebox (KK-011-AS, KOREA KIYON). EPR spectra of cobalt complexes were measured on an EMX plus continuous-wave X-band spectrometer equipped with a cryostat (Bruker). DLS measurements were performed with a Zetasizer Nano ZS instrument (Malvern Instruments Ltd., USA).

Synthesis of Co₂(OCOC₈F₁₇)₄((CH₃CH₂)₃NH·OCOC₈F₁₇)·(H₂O)₈. This compound was synthesized according to the synthetic procedure reported for Cu₂(OCOC₈F₁₇)₄ with some modifications.¹⁰ In brief, an acetone solution (30 mL) of CF₃(CF₂)₆CF₂CO₂H (1.4 g, 2.8 mmol) and triethylamine (0.56 g, 5.6 mmol) was stirred at room temperature for 30 min, and the unreacted triethylamine and solvent were evaporated. To the obtained residue were added acetone (30 mL) and

Co(ClO₄)₂·6H₂O (0.50 g, 1.4 mmol), and the mixture was stirred at room temperature for 30 min. After removal of the solvent, the mixture was extracted with TFT (15 mL × 5) and the TFT solution obtained was slowly evaporated to give the titled Co salt as a pink solid (0.84 g, 0.31 mmol, 45%). FAB-MS *m/z*: 522 [Co(OCOC₈F₁₇)₄]⁺, 964 [Co(OCOC₈F₁₇)₂ - F + 2H]⁺. IR (KBr): 1654, 1426, 1369, 1204, 1148 cm⁻¹. Anal. Calcd for (C₅₁H₃₂F₈₅N₁₀O₁₈Co₂)Co₂(OCOC₈F₁₇)₄[(CH₃CH₂)₃NH·OCOC₈F₁₇](H₂O)₈: C, 22.86; H, 1.20; N, 0.52. Found: C, 23.05; H, 1.33; N, 0.51. ¹H NMR (400 MHz, 298 K, (CD₃)₂CO) δ: 2.81 (q, 6H, NCH₂CH₃), 1.80 (t, 9H, NCH₂CH₃).

Synthesis of *N,N,N',N',N''*-Pentaoctyldiethylenetri-amine (C₈H₁₇-deta). This compound was prepared by a method similar to that used for the synthesis of the Rf-deta ligand. In brief, diethylenetriamine (0.16 g, 1.5 mmol), CH₃CN (40 mL), K₂CO₃ (1.6 g, 11 mmol), and *n*-octyl bromide (1.6 g, 8.5 mmol) were mixed in a three-necked flask under a nitrogen atmosphere, and the mixture was refluxed for 3 days. After cooling to room temperature, water (20 mL) was added to the resulting solution, and the mixture was extracted with chloroform (20 mL × 3). Removal of the solvent on a rotary evaporator gave the ligand as a yellow oil (0.20 g, 0.30 mmol, 20%). ¹H NMR (400 MHz, 298 K, CDCl₃) δ: 2.73–2.57 (m, 8H, NCH₂CH₂N), 2.51–2.35 (m, 10H, NCH₂(CH₂)₆CH₃), 1.46–1.36 (m, 10H, NCH₂CH₂(CH₂)₅CH₃), 1.26 (s, 50H, NCH₂CH₂(CH₂)₅CH₃), 0.88 (t, 15H, N(CH₂)₇CH₃). FAB-MS *m/z*: 666 [M + 2H]⁺. IR (KBr): 2926, 2854, 2253, 2197, 1467, 1378 cm⁻¹.

Catalytic Hydroxylation of Cyclohexane. Each reaction was conducted in a screw vial (*φ*: 12 mm, *H*: 35 mm) sealed with a silicone septum (Figure S2). Typically, a mixture of cyclohexane (550 μmol, 60 μL) and a solvent (140 μL of either CH₃NO₂, DMF, CH₃CN, CH₃CH₂CN, CHCl₃, or PFMCH) containing *m*-CPBA (32 μmol) was prepared and tightly sealed in the vial under a nitrogen atmosphere in a glovebox. After heating the sample to the requisite temperature, reactions were initiated by addition of a mixture of a ligand (9.4 nmol) and a metal salt (4.9 nmol) in 60 μL of TFT. After vigorous stirring of the solution at 50 °C for 2 h, the reaction was quenched by removal of the catalyst using a short silica gel column. TFT (1 mL) was then added to the solute to make the resulting solution homogeneous. Then, product analysis was performed using GC-FID. All peaks of interest were identified by comparing the retention times to those of the authentic samples. The product amounts were determined by comparison of their peak areas with that of an internal standard (nitrobenzene) using a calibration curve comprising a plot of mole ratio (moles of organic compound/mol of internal standard) vs area ratio (area of organic compound/area of internal standard). TONs of the catalyst were calculated based on the amount of cobalt ions. Data for hydroxylation reactions of other hydrocarbon substrates were corrected in a similar manner. Figure 2 was taken after the reaction in a 5-fold larger scale.

Determination of the Concentration of Cyclohexanol in the PFMCH/TFT System. PFMCH (700 μL), TFT (300 μL), cyclohexane (300 μL), *m*-CPBA (24 mg), and cyclohexanol (5–500 μL) were vigorously stirred in a vial at 50 °C. Standing the solution at 50 or 25 °C for 2 h without stirring, 100 μL of the solution was sampled from the bottom of the

vial, and then the amount of cyclohexanol in the sample totally homogenized by addition of TFT was analyzed by GC-FID.

Catalytic Hydroxylation of C5–C8 Alkanes. All procedures were carried out under the same conditions as those employed for the cyclohexane hydroxylation in a mixed solvent system, i.e., PFMCH and TFT in a 7:3 ratio (v/v). The resulting solution was analyzed by GC-FID or ^1H NMR after the reaction was quenched by removal of the catalyst using a short silica gel column. For ^1H NMR analysis of the products, 1,1,2,2-tetrachloroethane was employed as an internal standard.

Catalytic Hydroxylation of *n*-Butane. A butane-saturated solution of CH_3CN or PFMCH was prepared by gentle bubbling of gaseous *n*-butane into the solvent at 10°C . The concentration of butane in the solution was determined by ^1H NMR using 1,1,2,2-tetrachloroethane as an internal standard. After the addition of *m*-CPBA and the ligand, a sample vial was sealed, and the solution temperature was raised to 50°C . The reaction was initiated by the addition of the metal salt, and the reaction mixtures were stirred for 2 h. Then, the resulting mixture was analyzed by GC-FID and ^1H NMR. The typical set of conditions used is the same as those employed for the cyclohexane hydroxylation reaction.

■ ASSOCIATED CONTENT

SI Supporting Information

The Supporting Information is available free of charge at <https://pubs.acs.org/doi/10.1021/acsomega.4c01204>.

Cyclohexane oxidation with free radical species; plausible reaction mechanism for catalytic hydrocarbon hydroxylation; effects of the mixing ratio; comparison of catalytic reactivity and alcohol selectivity; concentration of cyclohexanol in the fluorous solvent system; inhibitory effects; catalytic hydroxylation of *n*-hexane; polarity of solvents; ^1H NMR spectrum; miscibility of PFMCH; DLS data; and EPR spectra (PDF)

■ AUTHOR INFORMATION

Corresponding Authors

Yuma Morimoto – Department of Molecular Chemistry, Division of Advanced Chemistry, Graduate School of Engineering, Osaka University, Suita, Osaka 565-0871, Japan; Present Address: Department of Chemistry School of Science, Tokyo Institute of Technology, Ookayama, Meguro-ku, Tokyo 152-8550, Japan; orcid.org/0000-0002-5209-266X; Email: y-morimoto@mls.eng.osaka-u.ac.jp

Shinobu Itoh – Department of Molecular Chemistry, Division of Advanced Chemistry, Graduate School of Engineering, Osaka University, Suita, Osaka 565-0871, Japan; Email: shinobu@mls.eng.osaka-u.ac.jp

Authors

Yuki Shimaoka – Department of Molecular Chemistry, Division of Advanced Chemistry, Graduate School of Engineering, Osaka University, Suita, Osaka 565-0871, Japan

Kosuke Fukui – Department of Molecular Chemistry, Division of Advanced Chemistry, Graduate School of Engineering, Osaka University, Suita, Osaka 565-0871, Japan

Complete contact information is available at:

<https://pubs.acs.org/doi/10.1021/acsomega.4c01204>

Funding

This work was supported by the JST (the CREST program, JPMJCR16P1 for S.I.), a Grant-in-Aid for challenging Exploratory Research (JP16K13963 for S.I.), a Grant-in-Aid for Scientific Research (B) (JP22H02095 for Y.M.), and a Grant-in-Aid for Young Scientists (16K17878 for Y.M.) from JSPS. Y.M. expresses thanks for the financial support provided by Ube Industries, Ltd., and Osaka University.

Notes

The authors declare no competing financial interest.

■ ACKNOWLEDGMENTS

We thank Dr. Tomoyoshi Suenobu for his kind help with DLS measurement.

■ REFERENCES

- (1) (a) Shilov, A. E.; Shul'pin, G. B. *Activation and Catalytic Reactions of Saturated Hydrocarbons in the Presence of Metal Complexes*; Springer, 2006. (b) Murai, S. *Activation of Unreactive Bonds and Organic Synthesis*; Springer, 2003. (c) Crabtree, R. H. Aspects of Methane Chemistry. *Chem. Rev.* **1995**, *95* (4), 987–1007. (d) *Heterogeneous Hydrocarbon Oxidation*; Warren, B. K., Oyama, S. T., Eds.; ACS Symposium Series; American Chemical Society, 1996. (e) Labinger, J. A. Selective alkane oxidation: hot and cold approaches to a hot problem. *J. Mol. Catal. A: Chem.* **2004**, *220* (1), 27–35. (f) Sheldon, R. *Metal-Catalyzed Oxidations of Organic Compounds: Mechanistic Principles and Synthetic Methodology Including Biochemical Processes*; Elsevier Science, 2012. (g) Godula, K.; Sames, D. C-H Bond Functionalization in Complex Organic Synthesis. *Science* **2006**, *312* (5770), 67–72.
- (2) (a) Bravo, A.; Bjorsvik, H.-R.; Fontana, F.; Minisci, F.; Serri, A. Radical Versus “Oxenoid” Oxygen Insertion Mechanism in the Oxidation of Alkanes and Alcohols by Aromatic Peroxides. New Synthetic Developments. *J. Org. Chem.* **1996**, *61* (26), 9409–9416. (b) Bunescu, A.; Lee, S.; Li, Q.; Hartwig, J. F. Catalytic hydroxylation of polyethylenes. *ACS Cent. Sci.* **2017**, *3* (8), 895–903. (c) Gross, Z.; Simkhovich, L. Hydroxylation of Simple Alkanes by Iodosylbenzene is Catalyzed More Efficiently by Second than by Third Generation Iron(III) Porphyrins. *Tetrahedron Lett.* **1998**, *39* (44), 8171–8174. (d) Groves, J. T.; Kruper, W. J.; Haushalter, R. C. Hydrocarbon Oxidations with Oxometalloporphinates. Isolation and Reactions of a (Porphinato)manganese(V) Complex. *J. Am. Chem. Soc.* **1980**, *102* (20), 6375–6377. (e) Hill, C. L.; Schardt, B. C. Alkane Activation and Functionalization Under Mild Conditions by a Homogeneous Manganese(III)porphyrin-iodosylbenzene Oxidizing System. *J. Am. Chem. Soc.* **1980**, *102* (20), 6374–6375. (f) Leising, R. A.; Norman, R. E.; Que, L. Alkane Functionalization by Nonporphyrin Iron Complexes: Mechanistic Insights. *Inorg. Chem.* **1990**, *29* (14), 2553–2555. (g) Sako, M.; Hirota, K.; Maki, Y. Photo-oxygenation of Alkanes by a Heterocyclic N-Oxide via Non-Oxene Mechanism. Peculiar Photochemical Property of Pyrimido[5,4-G]-preiridine N-Oxide. *Chem. Pharm. Bull.* **1990**, *38* (7), 2069–2071. (h) West, J. P.; Schmerling, L. The Peroxide-Induced Exchange of Hydrogen and Chlorine between Saturated Hydrocarbons and Polychloroalkanes. *J. Am. Chem. Soc.* **1950**, *72* (8), 3525–3527.
- (3) (a) Li, C. J.; Chan, T. H. *Comprehensive Organic Reactions in Aqueous Media*; Wiley, 2007. (b) Lindstrom, U. M. *Organic Reactions in Water: Principles, Strategies and Applications*; Wiley, 2008.
- (4) (a) Kirsch, P. *Modern Fluoroorganic Chemistry: Synthesis, Reactivity, Applications*; Wiley, 2013. (b) Sandford, G. Perfluoroalkanes. *Tetrahedron* **2003**, *59* (4), 437–454.
- (5) Ohkubo, K.; Hirose, K. Light-Driven C–H Oxygenation of Methane into Methanol and Formic Acid by Molecular Oxygen Using a Perfluorinated Solvent. *Angew. Chem., Int. Ed.* **2018**, *57* (8), 2126–2129.
- (6) Morimoto, Y.; Shimaoka, Y.; Ishimizu, Y.; Fujii, H.; Itoh, S. Direct Observation of Primary C-H Bond Oxidation by an Oxido-

- Iron(IV) Porphyrin pi-Radical Cation Complex in a Fluorinated Carbon Solvent. *Angew. Chem., Int. Ed.* **2019**, *58* (32), 10863–10866.
- (7) Scott, R. L. The Solubility of Fluorocarbons I. *J. Am. Chem. Soc.* **1948**, *70* (12), 4090–4093.
- (8) Horváth, I. T.; Rábai, J. Facile Catalyst Separation Without Water: Fluorous Biphasic Hydroformylation of Olefins. *Science* **1994**, *266* (5182), 72–75.
- (9) (a) de Castries, A.; Magnier, E.; Monmotton, S.; Fensterbank, H.; Larpent, C. An Expedient Synthesis of Perfluorinated Tetraazamacrocycles: New Ligands for Copper-Catalyzed Oxidation under Fluorous Biphasic Conditions. *Eur. J. Org. Chem.* **2006**, *2006* (20), 4685–4692. (b) Liu, C.; Shen, D.-M.; Chen, Q.-Y. Fluorous Biphasic Catalytic Oxidation of Alkenes and Aldehydes with Air and 2-Methylpropanal in the Presence of (β -Perfluoroalkylated tetraphenylporphyrin)cobalt Complexes. *Eur. J. Org. Chem.* **2006**, *2006* (12), 2703–2706. (c) Özer, M.; Yilmaz, F.; Erer, H.; Kani, I.; Bekaroglu, O. Synthesis, characterization and catalytic activity of novel Co(II) and Pd(II)-perfluoroalkylphthalocyanine in fluorous biphasic system; benzyl alcohol oxidation. *Appl. Organomet. Chem.* **2009**, *23* (2), 55–61. (d) Pillai, U. R.; Sahle-Demessie, E. Selective oxidation of alcohols by molecular oxygen over a Pd/MgO catalyst in the absence of any additives. *Green Chem.* **2004**, *6* (3), 161–165. (e) Vincent, J.-M.; Rabion, A.; Yachandra, V. K.; Fish, R. H. Fluorous biphasic catalysis. 2. Synthesis of fluoroonytailed amine ligands along with fluoroonytailed carboxylate synthons, $[M(C_8F_{17}(CH_2)_2CO_2)_2]$ ($M = Mn^{2+}$ or Co^{2+}): Demonstration of a perfluoroheptane soluble precatalyst for alkane and alkene functionalization in the presence of tert-butyl hydroperoxide and oxygen gas. *Can. J. Chem.* **2001**, *79* (5–6), 888–895. (f) Pozzi, G.; Cavazzini, M.; Quici, S.; Fontana, S. Metal Complexes of a Tetraazacyclotetradecane Bearing Highly Fluorinated Tails: New Catalysts for the Oxidation of Hydrocarbons under Fluorous Biphasic Conditions. *Tetrahedron Lett.* **1997**, *38* (43), 7605–7608. (g) Pozzi, G.; Cinato, F. Efficient aerobic epoxidation of alkenes in perfluorinated solvents catalysed by chiral (salen) Mn complexes. *Chem. Commun.* **1998**, No. 8, 877–878. (h) Pozzi, G.; Montanari, F.; Quici, S. Cobalt tetraarylporphyrin-catalysed epoxidation of alkenes by dioxygen and 2-methylpropanal under fluorous biphasic conditions. *Chem. Commun.* **1997**, No. 1, 69–70. (i) Fish, R. H. Fluorous Biphasic Catalysis: A New Paradigm for the Separation of Homogeneous Catalysts from Their Reaction Substrates and Products. *Chem.—Eur. J.* **1999**, *5* (6), 1677–1680. (j) Barthel-Rosa, L. P.; Gladysz, J. A. Chemistry in fluorous media: a user's guide to practical considerations in the application of fluorous catalysts and reagents. *Coord. Chem. Rev.* **1999**, *190–192*, 587–605. (k) Vincent, J.-M.; Contel, M.; Pozzi, G.; Fish, R. H. How the Horváth paradigm, Fluorous Biphasic Catalysis, affected oxidation chemistry: Successes, challenges, and a sustainable future. *Coord. Chem. Rev.* **2019**, *380*, 584–599. (l) Contel, M.; Izuel, C.; Laguna, M.; Villuendas, P. R.; Alonso, P. J.; Fish, R. H. Fluorous Biphasic Catalysis: Synthesis and Characterization of Copper(I) and Copper(II) Fluoroonytailed 1,4,7-Rf-TACN and 2,2'-Rf-Bipyridine Complexes—Their Catalytic Activity in the Oxidation of Hydrocarbons, Olefins, and Alcohols, Including Mechanistic Implications. *Eur. J. Chem.* **2003**, *9* (17), 4168–4178. (m) Vincent, J.-M.; Rabion, A.; Yachandra, V. K.; Fish, R. H. Fluorous Biphasic Catalysis: Complexation of 1,4,7- $[C_8F_{17}(CH_2)_3]_3$ -1,4,7-Triazacyclononane with $[M(C_8F_{17}(CH_2)_2CO_2)_2]$ ($M = Mn, Co$) To Provide Perfluoroheptane-Soluble Catalysts for Alkane and Alkene Functionalization in the Presence of t-BuOOH and O_2 . *Angew. Chem., Int. Ed.* **1997**, *36* (21), 2346–2349.
- (10) Motreff, A.; Correa da Costa, R.; Allouchi, H.; Duttine, M.; Mathonière, C.; Duboc, C.; Vincent, J.-M. Dramatic Solid-State Humidity-Induced Modification of the Magnetic Coupling in a Dimeric Fluorous Copper(II)–Carboxylate Complex. *Inorg. Chem.* **2009**, *48* (13), 5623–5625.
- (11) Even water/lower alcohol mixed solutions, which appear to be perfectly mixed on a macroscopic level, are known to be separated at the molecular level.
- (12) (a) Shin, D. N.; Wijnen, J. W.; Engberts, J. B. F. N.; Wakisaka, A. On the Origin of Microheterogeneity: A Mass Spectrometric Study of Dimethyl Sulfoxide–Water Binary Mixture. *J. Phys. Chem. B* **2001**, *105* (29), 6759–6762. (b) Dixit, S.; Crain, J.; Poon, W. C. K.; Finney, J. L.; Soper, A. K. Molecular segregation observed in a concentrated alcohol–water solution. *Nature* **2002**, *416* (6883), 829–832. (c) Guo, J. H.; Luo, Y.; Augustsson, A.; Kashtanov, S.; Rubensson, J. E.; Shuh, D. K.; Ågren, H.; Nordgren, J. Molecular Structure of Alcohol–Water Mixtures. *Phys. Rev. Lett.* **2003**, *91* (15), 157401. (d) Roney, A. B.; Space, B.; Castner, E. W.; Napoleon, R. L.; Moore, P. B. A Molecular Dynamics Study of Aggregation Phenomena in Aqueous n-Propanol. *J. Phys. Chem. B* **2004**, *108* (22), 7389–7401. (e) Ratajska-Gadomska, B.; Gadomski, W. Influence of confinement on solvation of ethanol in water studied by Raman spectroscopy. *J. Chem. Phys.* **2010**, *133* (23), 234505.
- (13) Recycling the catalyst through extraction of products and byproducts with MeCN, followed by the addition of the substrate and m-CPBA in TFT, initiated subsequent runs. However, a decrease in yields was observed, likely resulting from the dissociation of cobalt from its ligand facilitated by m-CBA.
- (14) Wilhelm, E.; Battino, R. Thermodynamic functions of the solubilities of gases in liquids at 25 deg. *Chem. Rev.* **1973**, *73* (1), 1–9.
- (15) (a) Shul'pin, G. B.; Süß-Fink, G.; Shul'pina, L. S. Oxygenation of alkanes with hydrogen peroxide catalysed by osmium complexes. *Chem. Commun.* **2000**, No. 13, 1131–1132. (b) Shul'pin, G. B.; Kirillova, M. V.; Shul'pina, L. S.; Pombeiro, A. J. L.; Karslyan, E. E.; Kozlov, Y. N. Mild oxidative alkane functionalization with peroxides in the presence of ferrocene. *Catal. Commun.* **2013**, *31*, 32–36. (c) Yiu, S.-M.; Wu, Z.-B.; Mak, C.-K.; Lau, T.-C. FeCl₃-Activated Oxidation of Alkanes by [Os(N)O₃]. *J. Am. Chem. Soc.* **2004**, *126* (45), 14921–14929. (d) Nagababu, P.; Yu, S. S. F.; Maji, S.; Ramu, R.; Chan, S. I. Developing an efficient catalyst for controlled oxidation of small alkanes under ambient conditions. *Catal. Sci. Technol.* **2014**, *4* (4), 930–935.
- (16) (a) Nagataki, T.; Tachi, Y.; Itoh, S. Ni^{II}(TPA) as an efficient catalyst for alkane hydroxylation with m-CPBA. *Chem. Commun.* **2006**, No. 38, 4016–4018. (b) Qiu, Y.; Hartwig, J. F. Mechanism of Ni-catalyzed oxidations of unactivated C(sp³)–H bonds. *J. Am. Chem. Soc.* **2020**, *142* (45), 19239–19248. (c) Morimoto, Y.; Hanada, S.; Kamada, R.; Fukatsu, A.; Sugimoto, H.; Itoh, S. Hydroxylation of Unactivated C(sp³)–H Bonds with m-Chloroperbenzoic Acid Catalyzed by an Iron(III) Complex Supported by a Trianionic Planar Tetradentate Ligand. *Inorg. Chem.* **2021**, *60*, 7641–7649. (d) Shinke, T.; Itoh, M.; Wada, T.; Morimoto, Y.; Yanagisawa, S.; Sugimoto, H.; Kubo, M.; Itoh, S. Revisiting alkane hydroxylation with m-CPBA (m-chloroperbenzoic acid) catalyzed by nickel(II) complexes. *Chem.—Eur. J.* **2021**, *27* (59), 14730–14737. (e) Balamurugan, M.; Mayilmurugan, R.; Suresh, E.; Palaniandavar, M. Nickel(II) complexes of tripodal 4N ligands as catalysts for alkane oxidation using m-CPBA as oxidant: ligand stereoelectronic effects on catalysis. *Dalton Trans.* **2011**, *40* (37), 9413–9424. (f) Nam, W.; Ryu, J. Y.; Kim, I.; Kim, C. Stereoselective alkane hydroxylations by metal salts and m-chloroperbenzoic acid. *Tetrahedron Lett.* **2002**, *43* (31), 5487–5490. (g) Nishiura, T.; Takabatake, A.; Okutsu, M.; Nakazawa, J.; Hikichi, S. Heteroleptic cobalt(III) acetylacetonato complexes with N-heterocyclic carbene-donating scorpionate ligands: synthesis, structural characterization and catalysis. *Dalton Trans.* **2019**, *48* (8), 2564–2568. (h) Sankaralingam, M.; Balamurugan, M.; Palaniandavar, M.; Vadivelu, P.; Suresh, C. H. Nickel(II) complexes of pentadentate N5 ligands as catalysts for alkane hydroxylation by using m-CPBA as oxidant: a combined experimental and computational study. *Chem.—Eur. J.* **2014**, *20* (36), 11346–11361. (i) Nagataki, T.; Itoh, S. Catalytic alkane hydroxylation reaction with nickel(II) complexes supported by di- and triphenol ligands. *Chem. Lett.* **2007**, *36* (6), 748–749. (j) Terao, I.; Horii, S.; Nakazawa, J.; Okamura, M.; Hikichi, S. Efficient alkane hydroxylation catalysis of nickel(II) complexes with oxazoline donor containing tripodal tetradentate ligands. *Dalton Trans.* **2020**, *49* (18), 6108–6118. (k) Hikichi, S.; Hanaue, K.; Fujimura, T.; Okuda, H.; Nakazawa, J.; Ohzu, Y.; Kobayashi, C.;

Akita, M. Characterization of nickel(II)-acylperoxy species relevant to catalytic alkane hydroxylation by nickel complex with mCPBA. *Dalton Trans.* **2013**, 42 (10), 3346–3356. (l) Nagataki, T.; Ishii, K.; Tachi, Y.; Itoh, S. Ligand effects on Ni^{II}-catalysed alkane-hydroxylation with m-CPBA. *Dalton Trans.* **2007**, No. 11, 1120–1128.

(17) Regardless of our trial, we could not obtain any information about the reactive species through resonance-Raman and ESI-mass measurement.

(18) The notably high KIE observed is indicative of hydrogen atom tunneling during the rate-determining step of the reaction, a phenomenon occasionally reported in studies for reactive-oxygen complexes of transition metals. Alternatively, it is possible that the C–H bond dissociation process. Competing with another reaction decreasing TON, which could escalate a typical KIE value.

(19) Nesterova, O. V.; Kuznetsov, M. L.; Pombeiro, A. J. L.; Shul'pin, G. B.; Nesterov, D. S. Homogeneous oxidation of C–H bonds with m-CPBA catalysed by a Co/Fe system: mechanistic insights from the point of view of the oxidant. *Catal. Sci. Technol.* **2022**, 12 (1), 282–299.

(20) Maciuk, S.; Wood, S. H.; Patel, V. K.; Shapland, P. D. P.; Tomkinson, N. C. O. Peracid Oxidation of Unactivated sp³ C–H Bonds: An Important Solvent Effect. *Chem.—Eur. J.* **2023**, 29 (31), No. e202204007.

(21) (a) Kunishita, A.; Ertem, M. Z.; Okubo, Y.; Tano, T.; Sugimoto, H.; Ohkubo, K.; Fujieda, N.; Fukuzumi, S.; Cramer, C. J.; Itoh, S. Active Site Models for the Cu_A Site of Peptidylglycine α -Hydroxylating Monooxygenase and Dopamine β -Monooxygenase. *Inorg. Chem.* **2012**, 51 (17), 9465–9480. (b) Tano, T.; Ertem, M. Z.; Yamaguchi, S.; Kunishita, A.; Sugimoto, H.; Fujieda, N.; Ogura, T.; Cramer, C. J.; Itoh, S. Reactivity of Copper(ii)-alkylperoxy Complexes. *Dalton Trans.* **2011**, 40 (40), 10326–10336. (c) Nam, W.; Lim, M. H.; Lee, H. J.; Kim, C. Evidence for the Participation of Two Distinct Reactive Intermediates in Iron(III) Porphyrin Complex-Catalyzed Epoxidation Reactions. *J. Am. Chem. Soc.* **2000**, 122 (28), 6641–6647. (d) Wang, B.; Lee, Y.-M.; Clémancey, M.; Seo, M. S.; Sarangi, R.; Latour, J.-M.; Nam, W. Mononuclear Nonheme High-Spin Iron(III)-Acylperoxy Complexes in Olefin Epoxidation and Alkane Hydroxylation Reactions. *J. Am. Chem. Soc.* **2016**, 138 (7), 2426–2436.

(22) Larson, V. A.; Battistella, B.; Ray, K.; Lehnert, N.; Nam, W. Iron and manganese oxo complexes, oxo wall and beyond. *Nat. Rev. Chem.* **2020**, 4, 404–419.

(23) (a) Wang, B.; Lee, Y.-M.; Tcho, W.-Y.; Tussupbayev, S.; Kim, S.-T.; Kim, Y.; Seo, M. S.; Cho, K.-B.; Dede, Y.; Keegan, B. C.; et al. Synthesis and reactivity of a mononuclear non-haem cobalt(IV)-oxo complex. *Nat. Commun.* **2017**, 8 (1), 14839. (b) Yang, J.; Dong, H. T.; Seo, M. S.; Larson, V. A.; Lee, Y.-M.; Shearer, J.; Lehnert, N.; Nam, W. The Oxo-Wall Remains Intact: A Tetrahedrally Distorted Co(IV)–Oxo Complex. *J. Am. Chem. Soc.* **2021**, 143 (41), 16943–16959.

(24) Considering the abundances in the reaction system and bond dissociation energies, cyclohexane in PFC phase is another good hydrogen donor. This process can be possible, however, produced cyclohexyl radical eventually abstract hydrogen from m-CPBA.

(25) BDE values for the corresponding C–H and O–H bonds in kcal mol⁻¹ unit; BDE_{C–H} of cyclohexane: 99.5, BDE_{C–H} of chlorobenzene 112.9, BDE_{O–H} of benzoic acid 107.3. The values are taken from ref 26.

(26) Luo, Y.-R. *Comprehensive Handbook of Chemical Bond Energies*; CRC Press, 2007.

(27) δ is derived from the molecular cohesive energy per unit volume, and related to the polarity and polarizability of the compounds; molecules with low polarity has smaller δ values. Compounds with similar δ values tend to be miscible. This parameter can describe the difference of solubilizing ability between fluorocarbons and alkanes. The other solvent parameters such as hydrogen bond donatability (α), hydrogen bond acceptability, relative permittivity, dipole moment, donor number are summarized in Table S5 together with δ values. See ref 28 also.

(28) (a) Barton, A. F. M. Solubility parameters. *Chem. Rev.* **1975**, 75 (6), 731–753. (b) Marcus, Y. The properties of organic liquids that are relevant to their use as solvating solvents. *Chem. Soc. Rev.* **1993**, 22 (6), 409–416. (c) Haynes, W. M. *CRC Handbook of Chemistry and Physics*, 95th ed.; CRC Press, 2014.

(29) DLS measurement suggest microscopic phase separation of cyclohexanol also occurs in CH₂Cl₂/TFT system, although the separation seems less obvious compared to the PFMCH/TFT solvent system. An addition of cyclohexanol (2.0 μ L) to CH₂Cl₂/TFT solvent (700/300 μ L) produced a peak indicating formation of droplets with mean diameter of 51 nm, which is similar to PFMCH/TFT system forming larger droplets around 106 nm by a cyclohexanol injection (Figure S3b,c). By contrast, CH₃CN/TFT system did not from any new peak with an addition of cyclohexanol (Figure S3d).

(30) Litwinienko, G.; Ingold, K. U. Solvent Effects on the Rates and Mechanisms of Reaction of Phenols with Free Radicals. *Acc. Chem. Res.* **2007**, 40 (3), 222–230.

(31) Although the strategy is totally different, highly fluorinated alcohol was utilized to improve alcohol product selectivity in ref 32.

(32) Sterckx, H.; Morel, B.; Maes, B. U. W. Catalytic Aerobic Oxidation of C(sp³)–H Bonds. *Angew. Chem., Int. Ed.* **2019**, 58 (24), 7946–7970.

(33) Fujisaki, H.; Okamura, M.; Hikichi, S.; Kojima, T. Selective alkane hydroxylation and alkene epoxidation using H₂O₂ and Fe(II) catalysts electrostatically attached to a fluorinated surface. *Chem. Commun.* **2023**, 59 (22), 3265–3268.

(34) Armarego, W. L. F. *Purification of Laboratory Chemicals*; Elsevier Science, 2017.

(35) De Campo, F.; Lastécouères, D.; Vincent, J.-M.; Verlhac, J.-B. Copper(I) Complexes Mediated Cyclization Reaction of Unsaturated Ester under Fluoro Biphasic Procedure. *J. Org. Chem.* **1999**, 64 (13), 4969–4971.